Title

A frequency study of a clamped-clamped pipe immersed in a viscous fluid conveying internal steady flow for use in energy harvester development as applied to hydrocarbon production wells

Authors

Kjolsing, Eric
Todd, Michael

Publication Date

2015-04-03

DOI

10.1117/12.2084368

Peer reviewed

A frequency study of a clamped-clamped pipe immersed in a viscous fluid conveying internal steady flow for use in energy harvester development as applied to hydrocarbon production wells

Eric Kjolsing*[a], Michael Todd[a]
[a]Structural Engineering Department; University of San Diego, California
9500 Gilman Drive, Mail Code 0085, La Jolla, CA 92093-0085

ABSTRACT

Hydrocarbon extraction companies are seeking novel methods to generate and store power in down hole applications. Specifically, a robust energy harvesting system, capable of withstanding the harsh environmental and operational demands at the bottom of production wells, is desired to power commercially available well monitoring devices. The wide variety of well configurations makes this a challenging problem. Although some variables relating to the production tube are well defined by American Petroleum Institute standards, other variables may vary widely and be time dependent, such as annulus fluid properties. A first order task, then, is to characterize and understand the dynamics of a well through a study of changes in natural frequency over the broad range of inputs possessing moderate to high uncertainty.

This paper presents the results of an analytical frequency study which illustrates the effect of a select set of variables on the first natural frequency of a producing well. Specifically, axial force effects, fluid flow effects, and hydrodynamic effects, by means of a hydrodynamic function, are investigated. Due to the nature of the hydrodynamic function, the model is derived in the frequency domain and solved using the spectral element method.

Keywords: Energy Harvesting, Dynamics, Flow-Induced Vibration, Viscous Fluid, Hydrocarbon Production, Oil Well, Hydrodynamic Function, Spectral Element Method

1. INTRODUCTION

Novel energy harvesters are sought to power down hole monitoring equipment in hydrocarbon production wells. Although several sources of energy are feasible, utilizing mechanical vibrations stemming from the kinetic energy of the produced fluid is a common strategy[1]-[5] . These conceptual harvesters are often structurally supported by the production string: the first step towards the optimal design of a down hole energy harvester is to understand the dynamics of the production string. Previous work has investigated the behavior of pipes conveying[6]-[9] including the effects of nonlinear terms[10] and unsteady flow[11]-[14]. These investigations, however, did not account for an external medium, such as a confined fluid, often found in the annulus of production wells. Investigations incorporating viscoelastic foundations have been carried out[15]-[18] but these models fail to account for inertial effects known to exist when a beam vibrates in a fluid[19]-[21].

By means of a parametric study, this paper investigates the effects of axial force, annulus fluid properties, and annulus geometry on the first natural frequency of a production string as the conveyed fluid flow is varied. A Euler-Bernoulli beam formulation is used to define the equation of motion which is solved using the spectral element method. The results of the study are intended to help in the characterization of the dynamics of production strings, the likely structural support for deployed energy harvesting systems.

2. MODELING THE IN-SITU ENVIRONMENT

The design of each hydrocarbon well is unique, taking into account reservoir depth, projected production rates, and other

* eric.kjolsing@gmail.com

variables. Each well is typically optimized for economy and thus there is no "standard" configuration with which to base a frequency study. Rather than investigate specific wells and attempt to generalize the results, a parametric study is employed which will shed light onto the effects of various parameters of interest. To initiate the study, and specifically one that is computationally feasible, several idealizations must be made. First, it is assumed that the energy harvester will be located adjacent to the in-line components (such as well monitoring equipment) that presumably will draw power from the harvester (see Figure 1). Second, the steel production casing, grout liner, and soil are assumed to provide a rigid boundary that is coaxial to the production string. The space between the production casing and production string (e.g. the annulus) is filled with a fluid that is assumed to be stagnant and single-phased. The production string (through which the reservoir fluid is extracted) is assumed to have a constant cross section, implicitly assuming that the coupling elements along the production string produce negligible changes in system stiffness and mass. The production string is assumed to be braced above and below the yet-to-be-designed energy harvester so as to limit amplified vibrations from damaging in-line components. This bracing will likely generate a boundary somewhere between a pinned-pinned and clamped-clamped condition (with the production string itself helping to prevent rotation). The boundary in this study is taken to be clamped-clamped for simplicity. Interested readers can repeat the described work with alternate end conditions in order to bound the solution, however, it is believed the trends produced by the following parametric study will be similar. Lastly, although multiphase fluid is common in oil wells, modeling multiphase flow is burdensome and considered unnecessary since the primary interest of this paper is the effects the annulus geometry and annulus fluid have on the system. As such, the conveyed fluid is assumed to be turbulent and is modeled as a plug flow with either average viscous or inviscid characteristics.

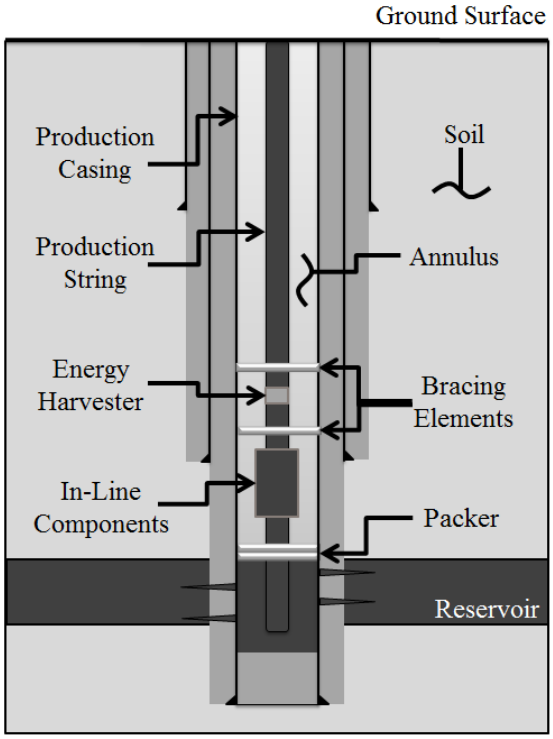

Figure 1. Modified well configuration

3. EQUATION OF MOTION

After neglecting gravity-induced tension effects and taking the fluid flow to be steady, the linearized equation of motion for a pipe conveying fluid[11] can be modified to include annulus fluid effects as

$$E^*I\dot{w}'''' + EIw'''' + \{M_iU^2 - \bar{T} + \bar{p}A_i(1-2\nu)\}w'' + 2M_iU\dot{w}' + (M_i+m)gw' + c\dot{w} + (M_i+m)\ddot{w} - f_{hydro} = 0, \quad (1)$$

where prime indicates a derivative with respect to x and dot indicates a derivative with respect to time. The terms represented in equation (1) are: Kelvin-Voigt dissipation, flexural restoring force, centrifugal force, applied tension, pressure induced tension, Coriolis force, gravity, viscous damping, inertia, and the hydrodynamic force stemming from the annulus fluid. The hydrodynamic forcing has been derived as[22]-[24]

$$f_{hydro} = -i\rho_e \pi d^2 \omega \Gamma U_0 e^{i\omega t}, \tag{2}$$

where the complex hydrodynamic function, Γ, is given in Appendix B. The real part of the hydrodynamic function increases the effective mass of the system in proportion to the displaced volume of annulus fluid. The imaginary part of the hydrodynamic function generates a viscous drag term proportional to the pipes transverse velocity[25]. Due to the hydrodynamic forcing's dependence on frequency, equation (1) is conveniently solved in the frequency domain using the spectral element method. A description of the method can be found in the literature[26],[27].

4. RESULTS AND DISCUSSION

A parametric study is performed to investigate the shifts in the first natural frequency of various systems as the conveyed fluid velocity is increased. The variables of interest are the axial force in the production string, the annulus geometry, and the annulus fluid properties. The numeric inputs used in the study are tabulated in Appendix C; they are considered reasonable but do not necessarily coincide with specific values that may be found in a producing well. In the figures that follow, the conveyed fluid velocity and the systems first natural frequency are normalized as

$$u = \sqrt{\frac{M_i}{EI}} UL \quad \text{and,} \quad \Omega = \sqrt{\frac{M_i+m}{EI}} \omega L^2. \tag{3}$$

4.1 Axial force

Three levels of axial force are investigated: 75kN tension (case I), an unloaded system (case II), and 150kN compression (case III). The first natural frequencies of these systems are plotted in Figure 2 as the conveyed fluid velocity is increased (the negative convention indicates fluid flow in the direction opposite gravity, e.g. upwards from the reservoir to the ground surface). The downward trend in the real part of the natural frequency ($Re[\Omega]$) with increasing velocity is due to the centrifugal force inducing a compression force in the system. Recalling the third and fourth terms in equation (1), the relationship between the two forces is noted: $\bar{T} \sim M_i U^2$. Thus, as the fluid velocity increases, the apparent compression in the system increases, resulting in the lowering of $Re[\Omega]$. For example, compare the unloaded system (case II) with the compression system (case III). The first natural frequency of the unloaded system under zero flow (22.37) and at the critical flow velocity (-6.28) agree with published data[28],[29]. At zero flow, the effect of the applied compression in case III is to reduce the natural frequency of the system as[30]

$$\Omega_c = \Omega \sqrt{1 + \bar{T}/P_{Euler}}\,. \tag{4}$$

Noting the Euler buckling load to be 685kN, the predicted natural frequency provided by equation (4) ($\Omega_c = 19.77$) agrees well with the SEM result of 19.84 (error = 0.3%). At the point of divergence instability ($Re[\Omega] = Im[\Omega] = 0$), the fluid flow and external tension have reached the Euler limit such that $P_{Euler} = M_i U_{Cr}^2 - \bar{T}$. The critical flow velocity for case III can then be calculated as $u_{Cr} = -5.55$, agreeing with the results shown in Figure 2.

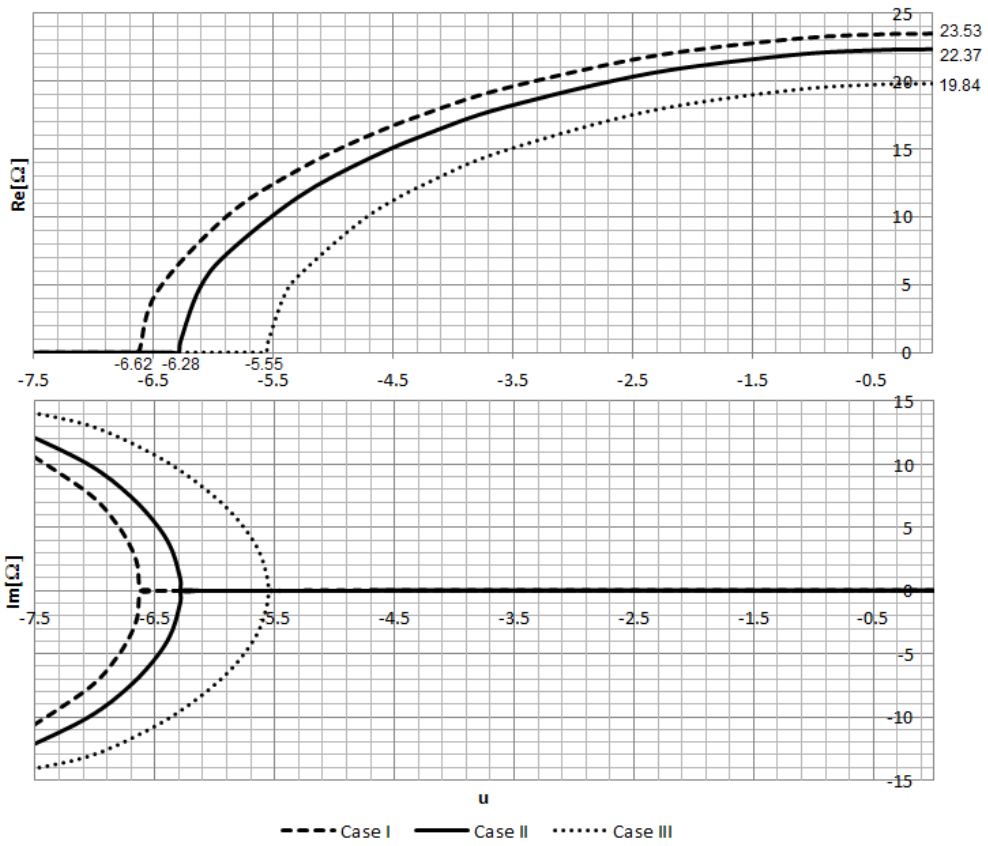

Figure 2. Flow velocity vs. fundamental frequency – axial force effects

4.2 Annulus fluid density

The annulus fluid density (ρ_e) arises in the hydrodynamic forcing and acts to scale the effects of the hydrodynamic function. Four cases are presented in Table 1 to illustrate the effects of the annulus fluid density. In each case, the flow velocity is taken to be zero and the hydrodynamic function is purely real. This later stipulation eliminates the viscous drag term that would arise for a viscous system (investigated later) resulting in only an added mass ($\rho_e \pi d^2 \Gamma_{real}$) to the four cases investigated here. By taking $\rho_e = 0$, case IV is equivalent to a pipe in a vacuum and results in the expected natural frequency at zero flow of $\Omega = 22.37$. The stiffness of the system can then be calculated as $K = \omega_n^2(M_i + m) = 86886\ kg/ms^2$. Cases V-VII have the same system stiffness which allows there natural frequencies to be directly calculated. By selecting various hydrodynamic functions and annulus fluid densities, the natural frequencies of the four systems can be calculated analytically and via the SEM procedure.

Table 1. Annulus fluid density effects

Case	Γ	$\rho_e \left(\frac{kg}{m^3}\right)$	$m_{added} \left(\frac{kg}{m}\right)$	Ω	
				Calculated*	SEM
IV	1	0	0.00	22.37	22.37
V	1	2500	38.48	16.11	16.11
VI	2	800	24.63	17.72	17.72
VII	3	1100	50.80	15.00	15.00

* $\Omega = \sqrt{\frac{K(M_i + m)}{EI(M_i + m + m_{added})}} L^2$

4.3 Annulus viscosity and geometry

The annulus viscosity and annulus geometry define the hydrodynamic function, which in turn, defines the hydrodynamic forcing. As previously stated, the real part of the hydrodynamic function generates added mass to the system while the imaginary part generates viscous drag. The following sections investigate how the annulus viscosity and annulus geometry shape the hydrodynamic function, followed by the effect the hydrodynamic function has on both an inviscid and a viscous system.

4.3.1 Hydrodynamic function

As noted in Appendix B, the hydrodynamic function is defined by the annulus viscosity (v_e), the outer radius of the production string (d), and the inner radius of the steel casing (D). Four different hydrodynamic functions are defined by the inputs listed in Table 2 and are plotted in Figure 3. The real part of the hydrodynamic function is dominated by D/d effects while the imaginary part has greater dependence on both the assumed geometry and viscosity.

Table 2. Hydrodynamic function inputs

		$\frac{D}{d}$	
		1.15	**1.25**
$v_e\left(\frac{m^2}{s}\right)$	**1.50E-04**	H1	H2
	1.50E-05	L1	L2

d=0.07m

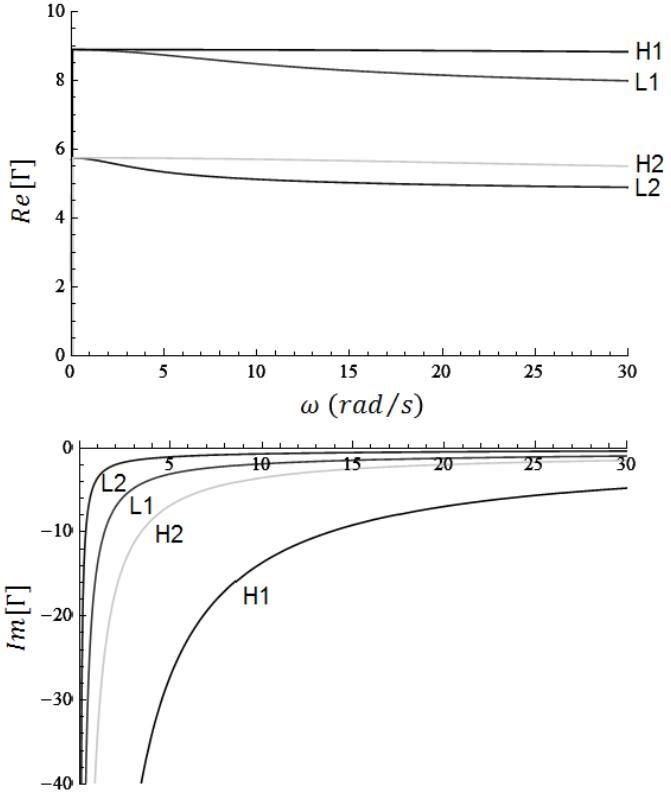

Figure 3. Real and imaginary parts of the hydrodynamic function for various inputs

4.3.2 Inviscid system

Assuming an inviscid fluid ($v_e = 0$) leads to a purely real hydrodynamic function which results in an added mass to the system. The first natural frequencies of three systems (cases VIII-X) with varying hydrodynamic functions are plotted in Figure 4. As the annulus fluid density is set to zero in case VIII, this case acts as a beam in vacuum benchmark. As the hydrodynamic function is increased (by reducing the D/d ratio) the real part of the hydrodynamic function increases (recall Figure 3). This results in an increasing added mass ($\rho_e \pi d^2 \Gamma_{real}$) and a predictable decrease in the systems natural frequency. Table 3 uses the system stiffness calculated previously ($K = 86886\ kg/ms^2$) to analytically calculate the natural frequency of the three cases. Unlike cases I-III (see Figure 2), cases VIII-X all share the same divergence point at $u_{Cr} = -6.28$. Since divergence is a static phenomenon, its occurrence is not dependent on inertial effects: added mass does not change the critical flow velocity.

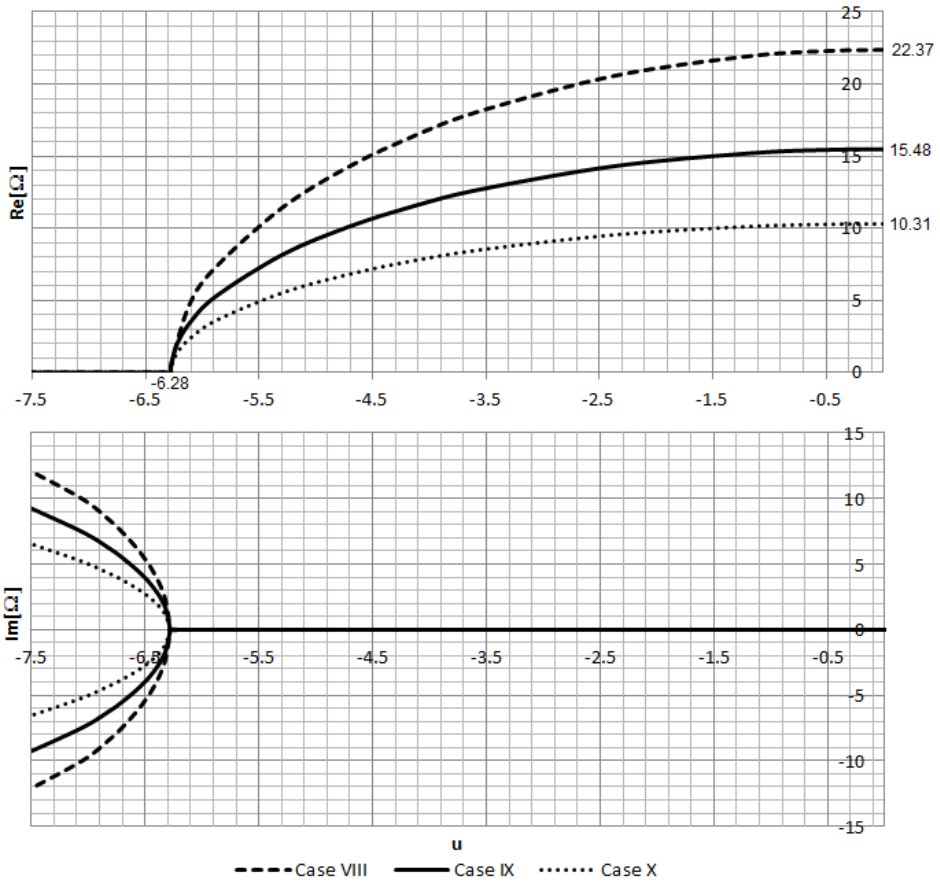

Figure 4. Flow velocity vs. fundamental frequency – inviscid system

Table 3. Effects of added mass with zero flow velocity

Case	Γ	$\rho_e \left(\frac{kg}{m^3}\right)$	$m_{added} \left(\frac{kg}{m}\right)$	Ω	
				Calculated*	SEM
VIII	1.00	0	0.00	22.37	22.36
IX	3.08	950	45.04	15.49	15.48
X	10.52	950	153.85	10.30	10.30

$* \Omega = \sqrt{\frac{K(M_i + m)}{EI(M_i + m + m_{added})}} L^2$

4.3.3 Viscous system

The effects of the full hydrodynamic function are displayed in Figure 5 using four cases (XI-XIV) with case IX representing the benchmark case of a pipe in a vacuum. In the viscous case, the vertical shift in the real part of the fundamental frequency is due to both the real and imaginary parts of the hydrodynamic function, contributing both added mass and viscous drag, respectfully. Compare cases XII and XIII for the zero flow condition: the added mass of case XII is greater than that of case XIII. If no other hydrodynamic effect were in play, the real part of the natural frequency of case XII should be lower than that of case XIII. However, the viscous drag associated with case XIII is much larger than case XII, acting to reduce the natural frequency of the system below that found in case XII.

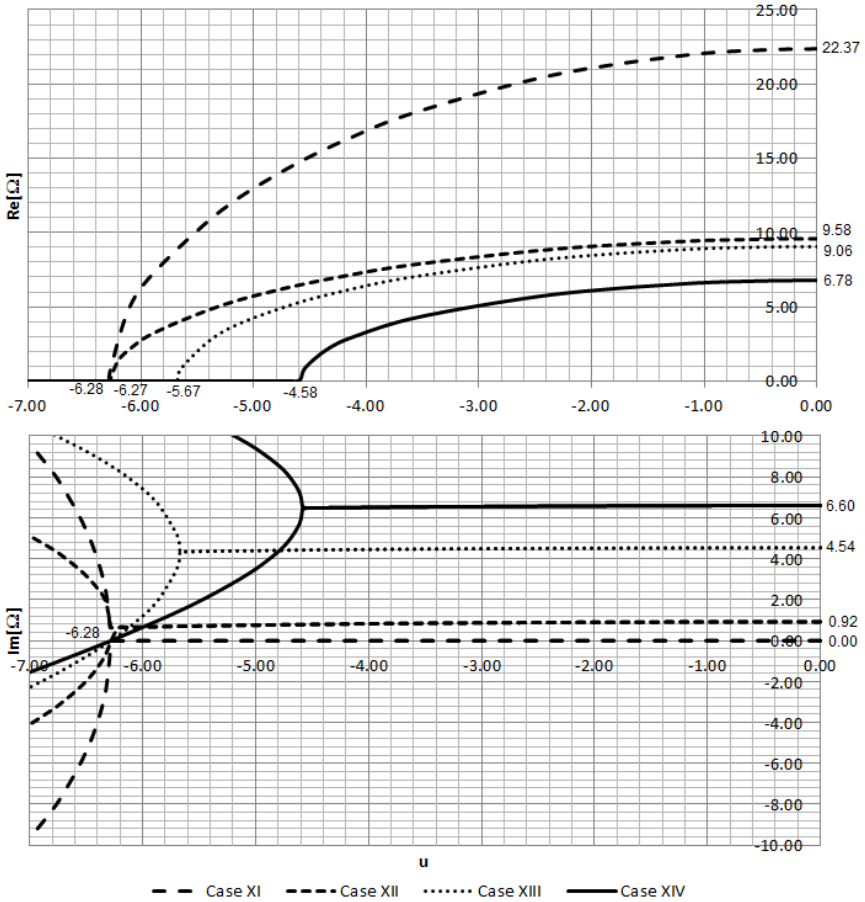

Figure 5. Flow velocity vs. fundamental frequency – viscous system

The bifurcation point (e.g. when $Re[\Omega] = 0$) marks the point where the system becomes overdamped and is visible on both plots of Figure 5. As the conveyed fluid velocity increases past this point, the complex natural frequency continues to migrate towards zero until divergence occurs ($Re[\Omega] = Im[\Omega] = 0$) and the system becomes unstable. The four cases shown have different bifurcation points due to the different levels of viscous drag (contributed by the imaginary part of the hydrodynamic function). However, all four cases have the same divergence point since, as previously mentioned, divergence is a static phenomenon leaving it independent of added mass and damping.

5. SUMMARY

An energy harvester is sought for down hole deployment in hydrocarbon production wells. To optimize the harvester, the dynamics of the supporting structure (e.g. the production string) must be well understood. To characterize the structural system, a parametric study was undertaken to investigate the effects of axial force, annulus geometry, and annulus fluid on a confined fluid conveying pipe as the produced fluid velocity was varied. The results of the study are

in-line with previously published research investigating analogous systems: (1) Axial force acts to stiffen (tension) or soften (compression) a system. (2) The annulus fluid density acts to scale the effects of the hydrodynamic function, which in turn, defines the hydrodynamic force. (3) The real part of the hydrodynamic function contributes added mass to the system while the imaginary part results in a viscous drag. (4) A shift in the bifurcation point is seen when either an axial force is included in the system or the annulus fluid is viscous. This study is a necessary step towards the development of a yet-to-be-designed energy harvester as the dynamics of the production string (investigated here) are expected to play a large role in the design of the energy harvester.

ACKNOWLEDGEMENTS

Funding was provided by Los Alamos National Laboratory through the Engineering Institute under Task 5 (Subcontract No. 77137-001-11).

REFERENCES

[1] Fripp, M. L. and Michael, R. K. (2007). *U.S. Patent No. 7,199,480*. Washington, DC: U.S. Patent and Trademark Office.
[2] Guerrero, J. C., Pabon, J. A., Auzerais, F. M., Chen, K. C. and Forbes, K. J. (2011). *U.S. Patent No. 7,906,861*. Washington, DC: U.S. Patent and Trademark Office.
[3] Pabon, J. A. and Bettin, G. (2013). *U.S. Patent No. 8,604,634*. Washington, DC: U.S. Patent and Trademark Office.
[4] Schultz, R. L., Michael, R. K., Robison, C. E. and Ringgenberg, P. D. (2004).*U.S. Patent No. 6,768,214*. Washington, DC: U.S. Patent and Trademark Office.
[5] Wetzel, R. J., Hiron, S., Veneruso, A. F., Patel, D. R., MacDougall, T. D. and Walter, J. (2009). *U.S. Patent Application 12/400,024*.
[6] Housner, G. W., "Bending vibrations of a pipe line containing flowing fluid," Journal of Applied Mechanics-Transactions of the ASME 19(2), 205-208 (1952).
[7] Long, R. H., "Experimental and theoretical study of transverse vibration of a tube containing flowing fluid," Journal of Applied Mechanics 77(1), 65-68 (1955).
[8] Dodds Jr, H. L. and Runyan, H. L. “Effect of high-velocity fluid flow on the bending vibrations and static divergence of a simply supported pipe,” No. NASA-TN-D-2870. National aeronautics and space administration Hampton VA Langley Research Center, 1965.
[9] Naguleswaran, S. and Williams, C. J. H., "Lateral vibration of a pipe conveying a fluid," Journal of Mechanical Engineering Science 10(3), 228-238 (1968).
[10] Lee, S. I. and Chung, J., "New non-linear modelling for vibration analysis of a straight pipe conveying fluid," Journal of Sound and Vibration 254(2), 313-325 (2002).
[11] Paidoussis, M. P. and Issid, N. T., "Dynamic stability of pipes conveying fluid," Journal of Sound and Vibration 33(3), 267-294 (1974).
[12] Lee, U., Pak, C. H. and Hong, S. C., "The dynamics of a piping system with internal unsteady flow," Journal of Sound and Vibration 180.2, 297-311 (1995).
[13] Seo, Y. S., Jeong, W.B., Jeong, S. H., Oh, J. S. and Yoo, W. S., "Finite element analysis of forced vibration for a pipe conveying harmonically pulsating fluid," JSME International Journal Series C 48(4), 688-694 (2005).
[14] Lee, U., and Park, J., "Spectral element modelling and analysis of a pipeline conveying internal unsteady fluid," Journal of Fluids and Structures 22(2), 273-292 (2006).
[15] Lottati, I. and Kornecki, A., "The effect of an elastic foundation and of dissipative forces on the stability of fluid-conveying pipes," Journal of Sound and Vibration 109(2), 327-338 (1986).
[16] Lee, U., Jang, I. and Go, H., "Stability and dynamic analysis of oil pipelines by using spectral element method," Journal of Loss Prevention in the Process Industries 22(6), 873-878 (2009).
[17] Soltani, P., Taherian, M. M., and Farshidianfar, A., "Vibration and instability of a viscous-fluid-conveying single-walled carbon nanotube embedded in a visco-elastic medium," Journal of Physics D: Applied Physics 43(42), 425401 (2010).
[18] Hosseini, M., Sadeghi-Goughari, M., Atashipour, S. A. and Eftekhari, M. "Vibration analysis of single-walled carbon nanotubes conveying nanoflow embedded in a viscoelastic medium using modified nonlocal beam model," Archives of Mechanics 66(4), 217-244 (2014).

[19] Tuck, E. O. "Calculation of unsteady flows due to small motions of cylinders in a viscous fluid," Journal of Engineering Mathematics 3(1), 29-44 (1969).
[20] Yeh, T. T. and Chen, S. S., "The effect of fluid viscosity on coupled tube/fluid vibrations," Journal of Sound and Vibration 59(3), 453-467 (1978).
[21] Siniavskii, V. F., Fedotovskii, V. S. and Kukhtin, A. B., "Oscillation of a Cylinder in a Viscous Liquid," Prikladnaia Mekhanika 16, 62-67 (1980).
[22] Stokes, G. G., [On the effect of the internal friction of fluids on the motion of pendulums. Vol. 9.], Pitt Press, (1851).
[23] Rosenhead, L., [Laminar Boundary Layers], Oxford: Clarendon Press, (1963).
[24] Wambsganss, M. W., Chen, S. S. and Jendrzejczyk, J. A., "Added mass and damping of a vibrating rod in confined viscous fluids," NASA STI/Recon Technical Report N 75, 10349 (1974).
[25] Cranch, G. A., Lane, J. E., Miller, G. A. and Lou, J. W., "Low frequency driven oscillations of cantilevers in viscous fluids at very low Reynolds number," Journal of Applied Physics 113(19), 194904 (2013).
[26] Doyle, J. F., [Wave propagation in structures], Springer US, (1989).
[27] Lee, U., [Spectral element method in structural dynamics], John Wiley & Sons, (2009).
[28] Paidoussis, M. P., [Fluid-structure interactions: slender structures and axial flow. Vol. 1], Academic press, (1998).
[29] Rao, S. S., [Vibration of continuous systems], John Wiley & Sons, (2007).
[30] Bolotin, V. V., [The dynamic stability of elastic systems], Holden-Day, Inc., (1974).

APPENDIX A – NOMENCLATURE

The terms used in this paper are listed in Table A.1

Table A.1. Nomenclature

Dimensional Terms		*Dimensional Terms (cont.)*	
c	Viscous Damping Coefficient	U	Mean Axial Flow Velocity
d	Pipe Outer Radius	U_{cr}	Critical Fluid Velocity
f_{hydro}	Hydrodynamic Force	$U_0 e^{i\omega t}$	Pipe Velocity
g	Coefficient of Gravity	ρ_e	Annulus Fluid Density
m	Mass per Unit Length of Pipe	ρ_i	Conveyed Fluid Density
m_{added}	Added Mass	ρ_p	Pipe Density
$\bar{p}$	Mean Pressure Differential	υ_e	Annulus Fluid Kinematic Viscosity
t	Time	ω	Radial Frequency
w	Lateral Deflection of the Pipe	ω_n	Natural Frequency
w_t	Pipe Wall Thickness		
A_i	Flow Area	*Dimensionless Terms*	
A_p	Pipe Cross Sectional Area		
D	Confining Shell Inner Radius	i	Imaginary Unit
E	Young's Modulus	u	Normalized Fluid Velocity
E^*	Kelvin-Voigt Viscosity	u_{cr}	Nondimensional Critical Fluid Velocity
I	Pipe Inertia	I_0, I_1, K_0, K_1	Modified Bessel Functions
K	System Stiffness	$Im[\,]$	Imaginary Part
L	Pipe Length	$Re[\,]$	Real Part
M_i	Mass per Unit Length of Conveyed Fluid	ν	Poisson Ratio
P_{Euler}	Euler Buckling Load	Γ	Hydrodynamic Function
$\bar{T}$	Externally Applied Tension	Ω	Normalized Natural Frequency
		Ω_c	Normalized Natural Frequency Adjusted for Compression

APPENDIX B – HYDRODYNAMIC FUNCTION

The hydrodynamic function can be written as

$$\Gamma = \frac{\Gamma_{num}}{\Gamma_{den}} - 1 = Re[\Gamma] - iIm[\Gamma], \tag{B.1}$$

where

$$\begin{aligned}\Gamma_{num} = {} & 2\alpha^2[I_0(\alpha)K_0(\beta) - I_0(\beta)K_0(\alpha)] - 4\alpha[I_1(\alpha)K_0(\beta) + I_0(\beta)K_1(\alpha)] \\ & + 4\alpha\gamma[I_0(\alpha)K_1(\beta) + I_1(\beta)K_0(\alpha)] - 8\gamma[I_1(\alpha)K_1(\beta) - I_1(\beta)K_1(\alpha)]\end{aligned} \tag{B.2}$$

and

$$\begin{aligned}\Gamma_{den} = {} & \alpha^2(1-\gamma^2)[I_0(\alpha)K_0(\beta) - I_0(\beta)K_0(\alpha)] \\ & + 2\alpha\gamma[I_0(\alpha)K_1(\beta) - I_1(\beta)K_0(\beta) + I_1(\beta)K_0(\alpha) - I_0(\beta)K_1(\beta)] \\ & + 2\alpha\gamma^2[I_0(\beta)K_1(\alpha) - I_0(\alpha)K_1(\alpha) + I_1(\alpha)K_0(\beta) - I_1(\alpha)K_0(\alpha)].\end{aligned} \tag{B.3}$$

The arguments to the hydrodynamic function are

$$\bar{k} = \sqrt{\frac{i\omega}{v_e}}; \quad \alpha = \bar{k}d; \quad \beta = \bar{k}D; \quad \gamma = \frac{d}{D}. \tag{B.4}$$

Assumptions used in the derivation of the hydrodynamic function include:

- The production string is concentric to a rigid cylindrical shell.
- The production string is an isotropic linearly elastic solid and cylindrical with a uniform cross section.
- The annulus fluid is assumed to have zero velocity at the rigid shell and a velocity that matches the production string at the fluid-string interface.
- The length between supports (e.g. L) greatly exceeds the diameter of the production string (e.g. 2d).
- The transverse displacement of the production string is small.
- The annulus fluid is homogeneous, Newtonian, and incompressible.

APPENDIX C – INPUTS

The numeric inputs used in the parametric study are shown in Table C.1

Table C.1. Parametric study inputs

		Case													
		Axial Force Effects			Annulus Fluid Density				Inviscid System			Viscous System			
Variable	Units	I	II	III	IV	V	VI	VII	VIII	IX	X	XI	XII	XIII	XIV
E^*	kg/ms	0			0				0			0			
E	N/m^2	2E+11			2E+11				2E+11			2E+11			
d	m	0.07			0.07				0.07			0.07			
w_t	m	0.01			0.01				0.01			0.01			
I	m^4	8.68E-06			8.68E-06				8.68E-06			8.68E-06			
A_p	m^2	4.08E-03			4.08E-03				4.08E-03			4.08E-03			
A_i	m^2	1.13E-02			1.13E-02				1.13E-02			1.13E-02			
ν	-	0			0				0			0			
ρ_p	kg/m^3	7800			7800				7800			7800			
m	kg/m	31.86			31.86				31.86			31.86			
g	m/s^2	9.81			9.81				9.81			9.81			
L	m	10			10				10			10			
ρ_i	kg/m^3	850			850				850			850			
ρ_e	kg/m^3	0			0	2500	800	1100	0	950		0	950		
D	m	∞			NA**				∞	1.4d	1.1d	∞	1.1d	1.12d	1.1d
v_e	m^2/s	0			NA**				0			0	1.5E-05	1.5E-04	
M_i	kg/m	9.61			9.61				9.61			9.61			
U	m/s	Varies*			0				Varies*			Varies*			
$\bar{T}$	N	7.5E+04	0	-1.5E+05	0				0			0			
$\bar{p}$	N/m^2	0			0				0			0			
c	kg/s	0			0				0			0			

**The flow velocity is taken to be negative, indicating flow in the direction opposite gravity.*

***Hydrodynamic function is hard coded to specified numeric values.*